VIA MEDICA

ORIGINAL ARTICLE

Folia Morphol.
Vol. 66, No. 4, pp. 296–302

ISSN 0015–5659
www.fm.viamedica.pl

Distribution of neuronal nitric oxide synthase (nNOS)-immunoreactive elements in the rabbit piriform cortex

S. Wójcik, E. Spodnik, J.H. Spodnik, J. Dziewiątkowski, J. Moryś

Department of Anatomy and Neurobiology, Medical University, Gdańsk, Poland

[Received 14 August 2007; Revised 17 October 2007; Accepted 17 October 2007]

The piriform cortex (PC), the primary olfactory cortex, is involved in the processes of learning and stress response and possibly plays an important role in epileptogenic activity. The results of several recent studies suggest that those PC neurons that contain neuronal nitric oxide synthase (nNOS) may play a key role during spatial learning and in the modulation of initiation, propagation and generalisation of seizures in various experimental models and may influence neuronal vulnerability after epileptic insults. The aim of this study was to characterise the pattern of distribution and morphology of nNOS-immunoreactive elements in PC of the adult rabbit. The co-localisation of nNOS and calretinin (CR) was also studied. The pattern of nNOS-ir within the rabbit PC is similar to that described previously in other mammals. The morphology of nNOS-ir elements, namely varicose fibres and Cajal-Retzius cells, suggest that NO has an important influence on PC function. Surprisingly, in the rabbit PC nNOS-ir elements show a very low level of co-localisation with CR-ir.

Key words: neuronal nitric oxide synthase, calretinin, piriform cortex, rabbit, morphology

INTRODUCTION

The piriform cortex (PC) receives direct connections from the olfactory bulb and is engaged in olfactory perception and discrimination. In addition, PC possesses numerous reciprocal connections with other structures belonging to the limbic system, such as the amygdaloid complex, the subiculum and the entorhinal cortex [18], and is linked to spatial memory processing, stress response [2, 10] and the spreading of excitatory waves. The last aspect of PC's role in particular has been intensively studied and PC is commonly used in many experimental models of epilepsy, for example the kindling model of temporal lobe epilepsy with complex partial seizures [18] or LiCl/pilocarpine-induced *status epilepticus* [4]. The results of several studies suggest that those PC neurons that contain nitric oxide synthase (NOS) may play a key role in PC function during spatial learning [19]. They may also modulate initiation, propagation and generalisation of seizures in various experimental models and can influence neuronal vulnerability after epileptic insults [5, 17].

The NOS family comprises four main isoforms: neuronal (nNOS, known also as NOS I), endothelial (eNOS), inducible (inNOS) and mitochondrial (mtNOS). The synthesis of nitric oxide (NO) occurs during conversion of L-arginine to L-citrulline. NO produced by neurons works as a neurotransmitter, and its effect may be beneficial but also detrimental [6, 15]. It causes nitration, nitrosylation or oxidation of proteins, and subsequently influences several cellular mechanisms. The NO intracellular signalling involves the activation of guanylate cyclase, interaction with MAP kinases, apoptosis-related proteins

Address for correspondence: S. Wójcik, MD, PhD, Department of Anatomy and Neurobiology, Medical University of Gdańsk, Dębinki 1, 80–211 Gdańsk, Poland, tel: +48 58 349 14 01, fax: +48 58 349 14 21, e-mail: swoj@amg.gda.pl

and anti-proliferative molecules. It also plays a role in the post-translational modification of proteins and proteasome-dependent protein degradation [6, 8]. Moreover, under pathophysiological conditions such as in Parkinson's disease or Alzheimer's disease, NO causes cell damage through the formation of highly reactive peroxynitrite [22].

We have previously described the distribution and morphology of elements containing three calcium-binding proteins (CaBPs): parvalbumin, calbindin-D28k and calretinin (CR) in the adult rabbit PC [25]. We now intend to broaden our study of this commonly used laboratory animal with a characterisation of nNOS immunoreactivity (-ir) and its relation to CR-ir in PC.

MATERIAL AND METHODS

Five adult New Zealand rabbits were used in the study. The animal care and treatment were in accordance with the guidelines for laboratory animals established by the National Institute of Health, as well as those enforced by the local ethics committee. To obtain brain section for the immunohistochemical staining we followed a previously published protocol [24, 25]. Briefly, animals were deeply anaesthetised intraperitoneally with fentanyl and thiopental (0.03 mg/kg and 80 mg/kg, respectively). Next, they were transcardially perfused with 0.9% saline containing 10,000 units of heparin, followed by 4% solution of paraformaldehyde in phosphate buffer (pH 7.4, 4°C). Directly after perfusion the brains were taken out of the skulls and cryoprotected initially in 15% and subsequently in 30% sucrose phosphate buffer solution (pH 7.4, 4°C). After the brains had been soaked in the solution (1–3 days), they were cut on the cryostat (Jung 1800, Leica, Germany) into 40 μm thick coronal sections. Eight adjacent sections were taken every 1200 μm.

Immunohistochemistry

Free-floating sections were blocked in 3% normal goat serum (NGS; for NeuN and nNOS) or 3% normal donkey serum (NDS; for double staining NOS/calretinin), and 0.3% Triton X-100 in 0.01M PBS (pH 7.2) for 1 hour at room temperature. Next they were incubated with primary antibodies: mouse monoclonal anti-NeuN (Chemicon, USA; 1:500) or mouse monoclonal anti-nNOS (Sigma, USA; 1:500) or, for double staining, a cocktail of mouse monoclonal anti-nNOS and goat policlonal anti-calretinin (Chemicon, USA; 1:500) in 0.01 M PBS (pH 7.2) containing NGS and NDS and 0.1% Triton X-100 in 4°C. After 48 hours the sections were washed with PBS and incubated for 2 hours, room temperature with secondary goat anti-mouse antibody coupled with Cy3 (Jackson, USA; 1:800) or, for double staining, with a cocktail of donkey anti-mouse antibody coupled with Cy3 and donkey anti-goat antibody coupled with Alexa-488. Finally they were washed with PBS, mounted onto gelatin-coated slides, air dried and cover-slipped with Kaiser's gelatin (Merck, Germany). Omission of the primary antibody during control experiments results in absence of a signal.

Analysis

The low magnification imaging and initial analysis of immunostained sections were performed on a fluorescent microscope (Eclipse 600, Nikon, Japan) equipped with a digital camera (ColorView II, Olympus, Japan). Distribution of the nNOS-ir cells in particular layers of the PC was evaluated by two independent investigators. All nNOS-ir cells present on the given coronal section were counted. The high magnification imaging and co-localisation study were carried out using a confocal laser scanning microscopy (CLSM) system (Radiance 2100, Bio-Rad, United Kingdom) mounted on a microscope (Eclipse 600, Nikon, Japan). The CLSM images were obtained with 40x and 60x oil immersion objective lenses of N.A. = 1.3 and 1.4, respectively. The optimal iris was used for each magnification. The CLSM images were analysed with LaserSharp 2000 and LaserPix v. 2.0 software (both Bio-Rad, United Kingdom).

RESULTS

Partitioning and analysis of the laminar structure of the rabbit PC used in the present study were based on our previous studies [25], the results of which corresponded with a widely accepted description of the rat PC [7]. Both parts of PC, anterior and posterior, consisted of three layers: I — the superficial plexiform layer, II — the superficial compact cell layer and III — the deep cell layer. Because of the specific morphology of the dense bands of fibres [25] a subpial superficial portion (Ia) and a deep portion (Ib) are distinguished within layer I.

Distribution and morphology of nNOS immunoreactive elements

The immunoreactivity of nNOS in the anterior and posterior parts of PC was similar (Fig. 1A–D). nNOS-ir elements were heterogeneously distributed through

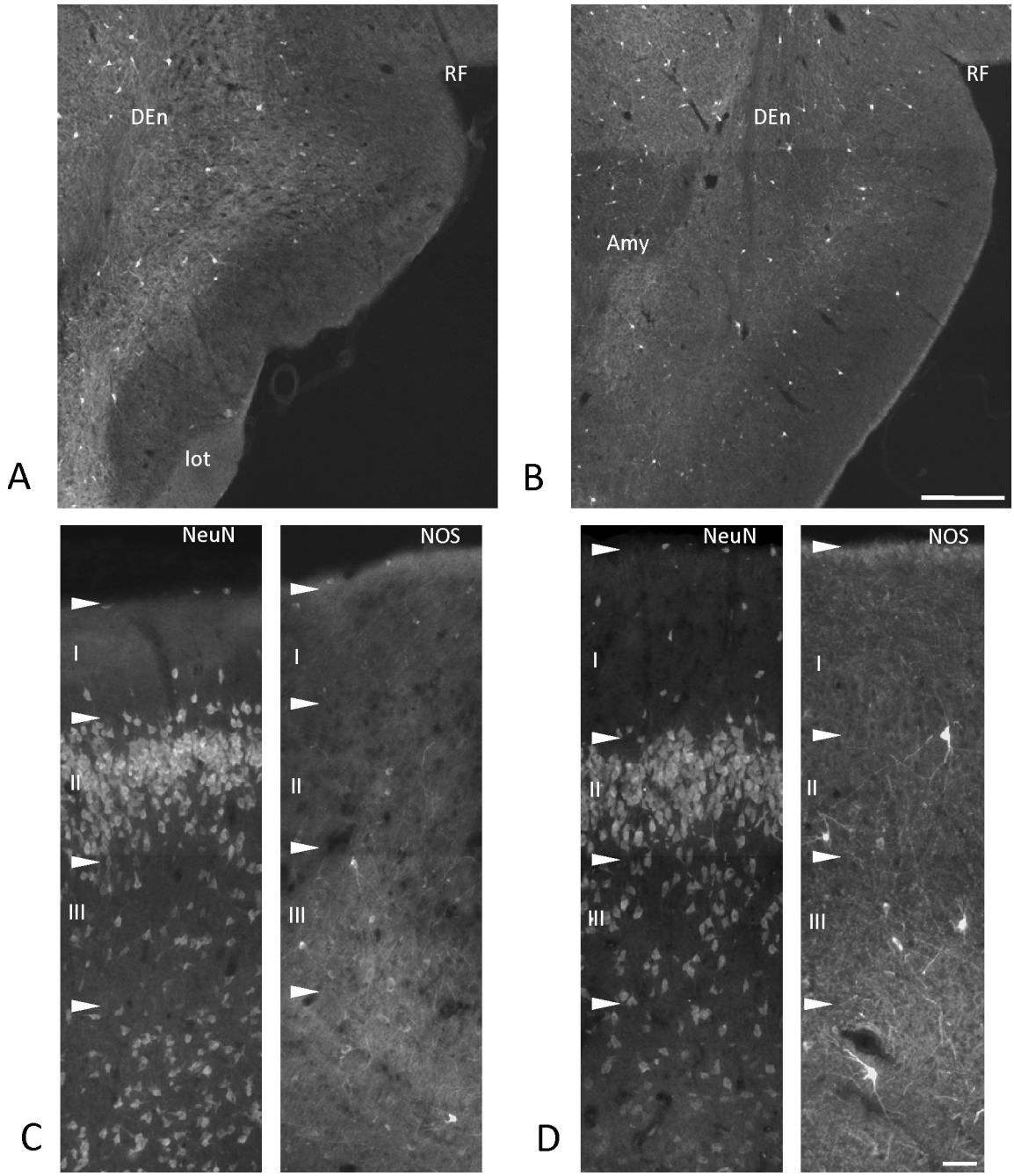

Figure 1. Photomicrographs show nNOS-immunoreactivity in the rabbit piriform cortex. **A**, **C** — anterior piriform cortex, **B**, **D** — posterior piriform cortex. The adjacent antiNeuN stained sections were used for determining the laminar division of the piriform cortex; Amy — amygdaloid complex; DEn — dorsal endopiriform nucleus; lot — lateral olfactory tract; RF — rhinal fissure; NeuN — neuron-specific protein; NOS — neuronal nitric oxide synthase (scale bar **A**, **B** — 500 μm; **C**, **D** — 50 μm).

the PC layers. The strongest nNOS-ir of neuropil in relative terms was observed in the most superficial layer, namely Ia, and in the deepest layer, layer III. Neurons containing nNOS were also located mainly in layers I and III of PC, amounting to 36% and 42%, respectively of the total number of stained neurons, while in layer II they only made up 23% (details in Table 1).

In layer Ia the nNOS-ir neurons usually had oval somata, and only sporadically were the proximal parts of processes visible (Fig. 2A). The long axes of the neuronal bodies were oriented parallel to the brain surface. In contrast, in layer Ib the oval somata of nNOS-ir neurons were mostly oriented with their long axes perpendicularly to the brain surface. In layer II nNOS-ir neurons with triangular cell bodies

Table 1. The distribution of neurons containing neuronal nitric oxide synthase (nNOS) and calretinin (CR) in layers of the rabbit piriform cortex

	nNOS (%)			CR (%)		
	I	II	III	I	II	III
Rb 1	32	26	41	19	67	15
Rb 2	23	28	49	17	73	11
Rb 3	37	25	38	34	57	9
Rb 4	37	24	39	6	78	16
Rb 5	49	11	41	40	56	4
Ave	**36**	**23**	**42**	**23**	**66**	**11**
SD	9	7	4	14	10	5

and clearly visible processes were observed. In layer III two distinct populations of nNOS-ir neurons were present, weakly stained round cells with almost no stained processes and polygonal darkly stained neurons with clearly visible processes (Fig. 2A). The polygonal neurons were also the largest of the nNOS-ir neurons in the rabbit PC (details in Table 2). nNOS-ir fibres also showed differentiated morphology and spatial orientation (Fig. 2B). Within layer Ia a dense network of thin fibres were observed, mostly oriented parallel to the brain surface. In contrast, in the inner portion of layer I smooth and varicose fibres oriented perpendicularly to the brain

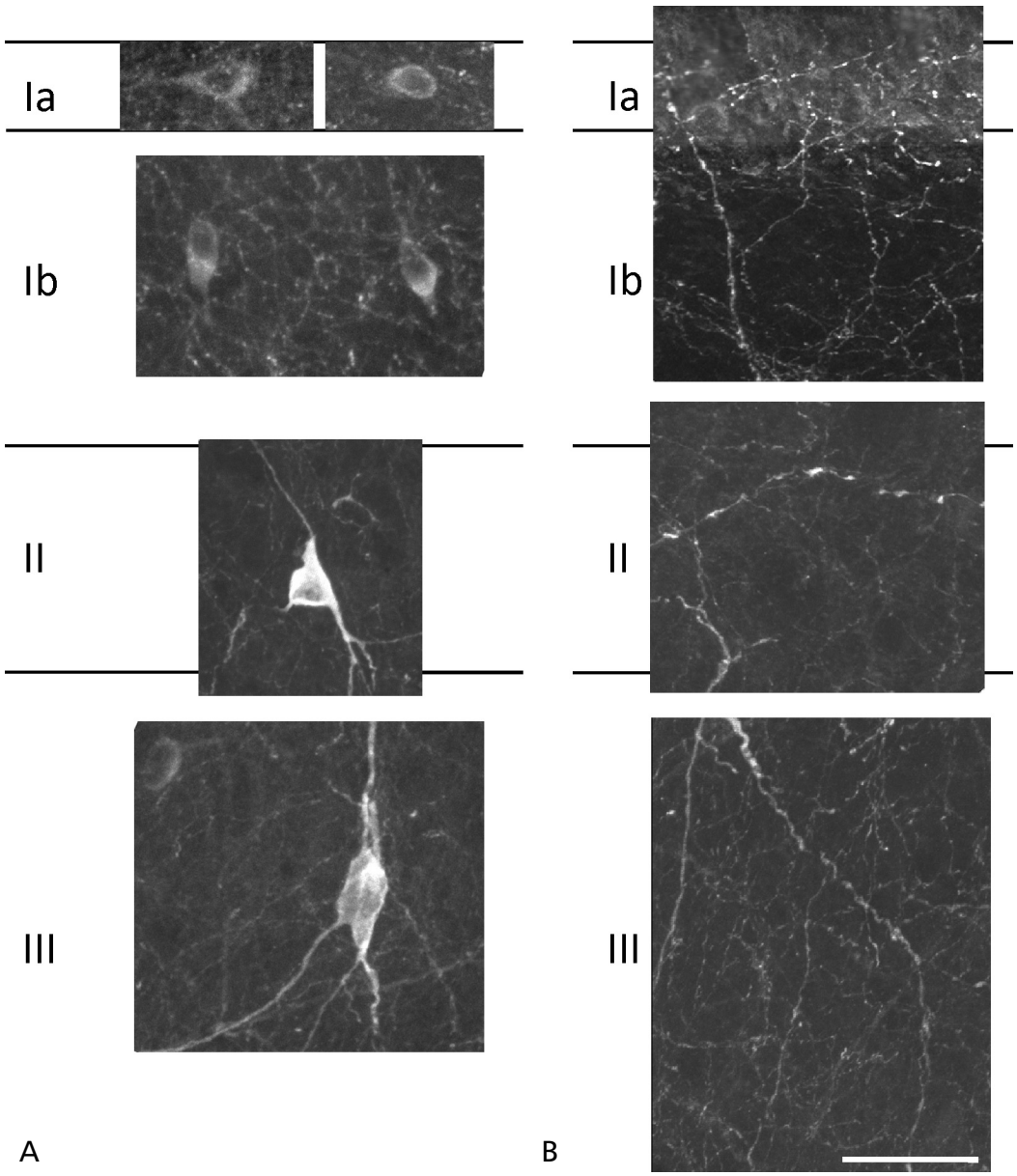

Figure 2. Photomicrographs show the morphology of nNOS-immunoreactive cells (**A**) and fibres (**B**) in particular layers of the piriform cortex (scale bar — 25 μm).

Table 2. nNOS-immunoreactive cell bodies within the rabbit piriform cortex (PC) characterised by shape and size

PC layer	Shape of soma	Long axis [μm]	Short axis [μm]	Area [μm^2]
Ia	Oval	15.0 ± 2.6	9.7 ± 1.2	108.7 ± 26.2
Ib	Oval	18.2 ± 1.5	11.4 ± 2.0	154.5 ± 19.9
II	Triangular	19.5 ± 3.0	13.1 ± 2.0	187.7 ± 43.5
III	Poligonal	30.2 ± 8.1	13.5 ± 2.7	306.1 ± 74.2
III	Round	17.8 ± 2.8	12.8 ± 1.6	169.0 ± 52.8

surface predominated. In layer II very thin nNOS-ir fibres surrounded unlabelled cell bodies, and thicker fibres with varicosities were found. In layer III numerous fibres (mostly distal parts of the processes of polygonal nNOS-ir neurons) were oriented in different directions. Fibres with varicosities were also observed here (Fig. 2B).

Double staining nNOS/calretinin

Because the morphology of nNOS-ir elements in layer I closely resembled CR-ir elements [25], and in view of the fact that co-localisation of those two proteins within the neighbouring structures has been described previously [12, 13] and has also been reported on recently within the olfactory structures [11], we decided to examine their interrelationship in the rabbit PC. The pattern of distribution and morphology of CR-ir elements in PC in double-stained sections was identical to that described previously [25]. We have extended the former study by quantifying the distribution of CR-ir neurons (Table 1).

In all the layers nNOS-ir and CR-ir elements predominantly comprised separate populations. A very small number of neurons containing both nNOS and CR was observed (Fig. 3A–F). The co-localisation with CR was observed in all subpopulations of nNOS neurons except the polygonal nNOS neurons in layer III (Fig. 3B, D, F). Of the nNOS neurons in layer I only 2.6% also showed CR-ir (n = 228), in layer II — 8.5% (n = 164), while in layer III this stood at 2.8% (n = 282). Within CR-ir neuron population, 6.0% of neurons in layer I (n = 100), 4.2% in layer II (n = 334), and 14.8% in layer III (n = 54) showed also nNOS-ir. nNOS-ir fibres were frequently located near the CR-ir cells and fibres (Fig. 3), but no co-localisation was observed within fibres.

DISCUSSION

The pattern of nNOS-ir within the piriform cortex is similar among mammals

Our study is the first detailed description of the distribution and morphology of nNOS-ir elements within PC of the adult rabbit, apart from work to which there is only limited access (an article in Chinese) and where the focus is on quantitative rather than qualitative data [16]. The results presented by us are similar to those previously reported in mice [21] and rats [26]. Moreover, taking into account the fact that qualitative and quantitative evaluation of cortical NADPH diaphorase (NADPH-d) and nNOS containing neurons revealed that more than 95% of these cells contained both enzymes [21], we may compare our results with data obtained from the PC of platypus and echidna [1], tenrec (Madagascan tree hedgehog) [14], hamster and rat [3], and cat [20]. Laminar distribution and morphology of NADPH-d containing neurons reported in all these species show a broad similarity to the distribution and morphology of nNOS-ir neurons in the rabbit PC described by us.

The morphology of nNOS-ir elements suggest their important influence on PC function

The varicose fibres observed in all the layers of the rabbit PC nNOS-ir and the neurons present in layer Ia enable some aspects of NO influence on PC neurons to be explained.

The varicosities are linked to one of the forms of paracrine neurotransmission, namely volume transmission, a process mediated via short distance diffusion of the neurotransmitter (e.g. 5HT) in the extracellular space [23]. It has been reported that NO, by virtue of its diffusion in extracellular space, can interact with synapses that are near the synthesis site but not necessarily anatomically connected to NO source by a conventional synaptic linkage [9]. The presence of fibres with varicosities in all layers suggests that the whole area of PC might be under NO influence.

Because of their particular location and the presence of morphological features neurons in layer Ia [19, 25] may by classified as Cajal-Retzius cells. In PC the functional targets of Cajal-Retzius cells are the terminal dendritic bouquets of projective cells [19]. It has recently been reported that cells in layer Ia may synthesise and release NO via a dense plexus of axonal branches and that leads to elimination by triggering apoptosis in the cortical projection neurons

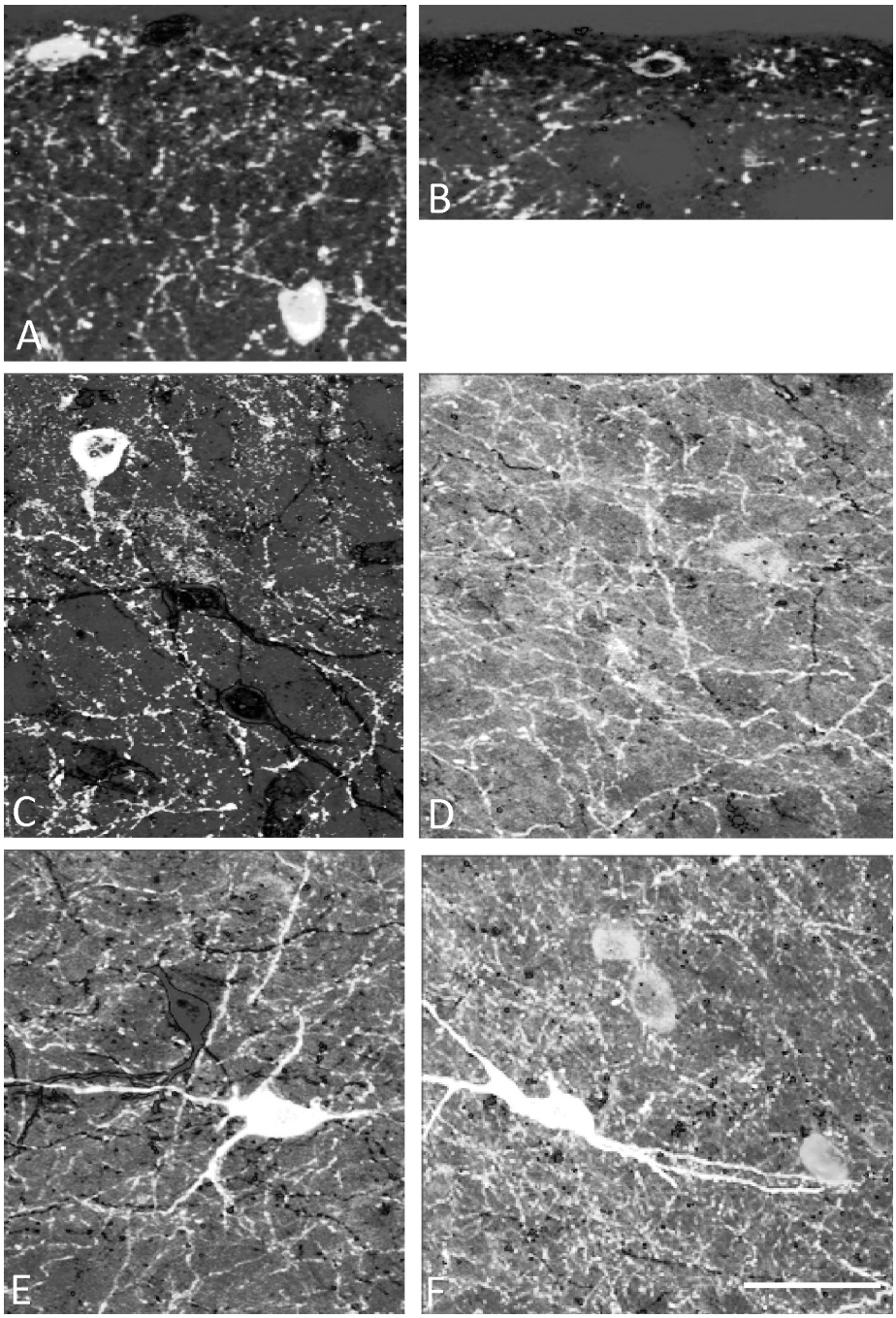
A
B
C
D
E
F

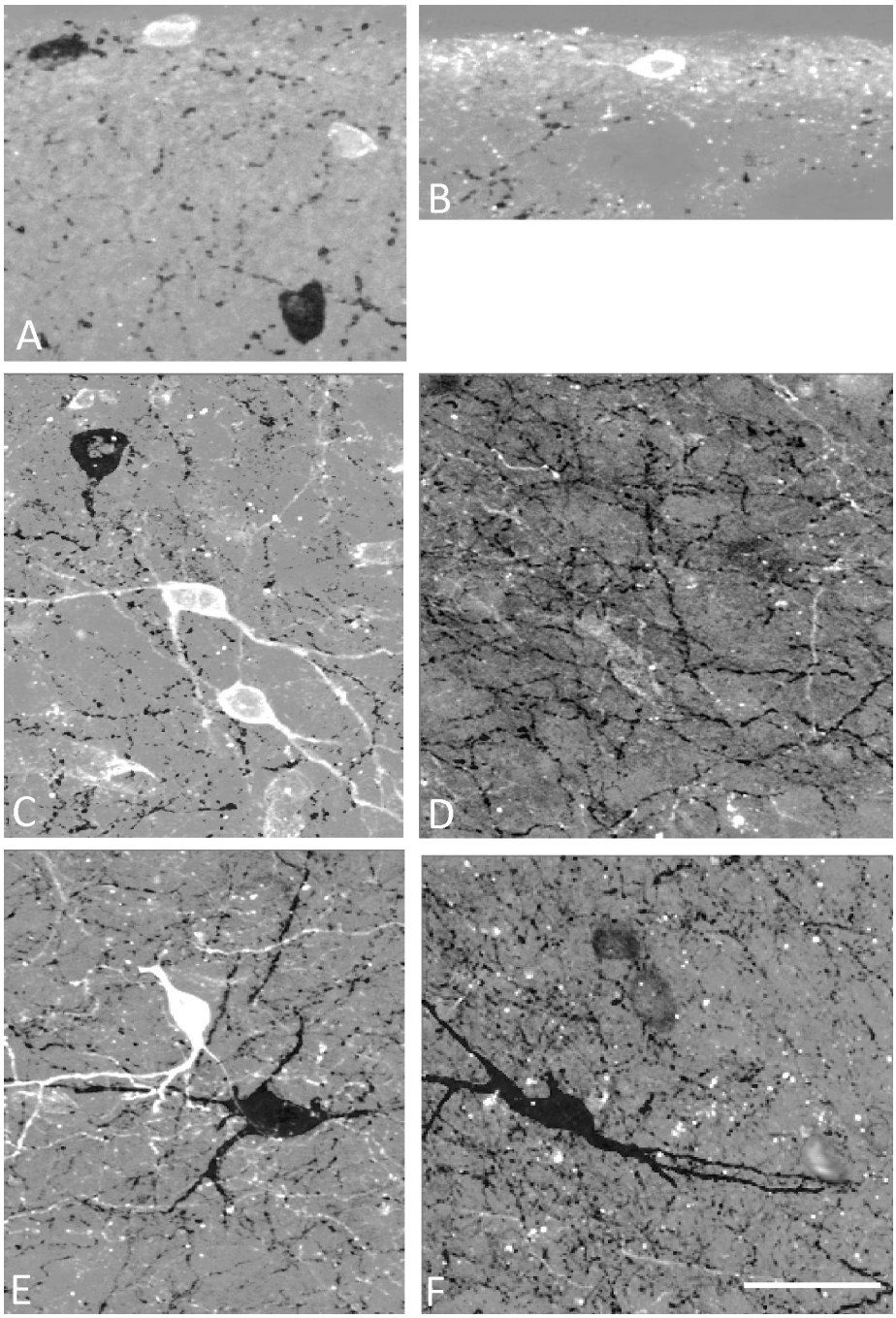
A
B
C
D
E
F

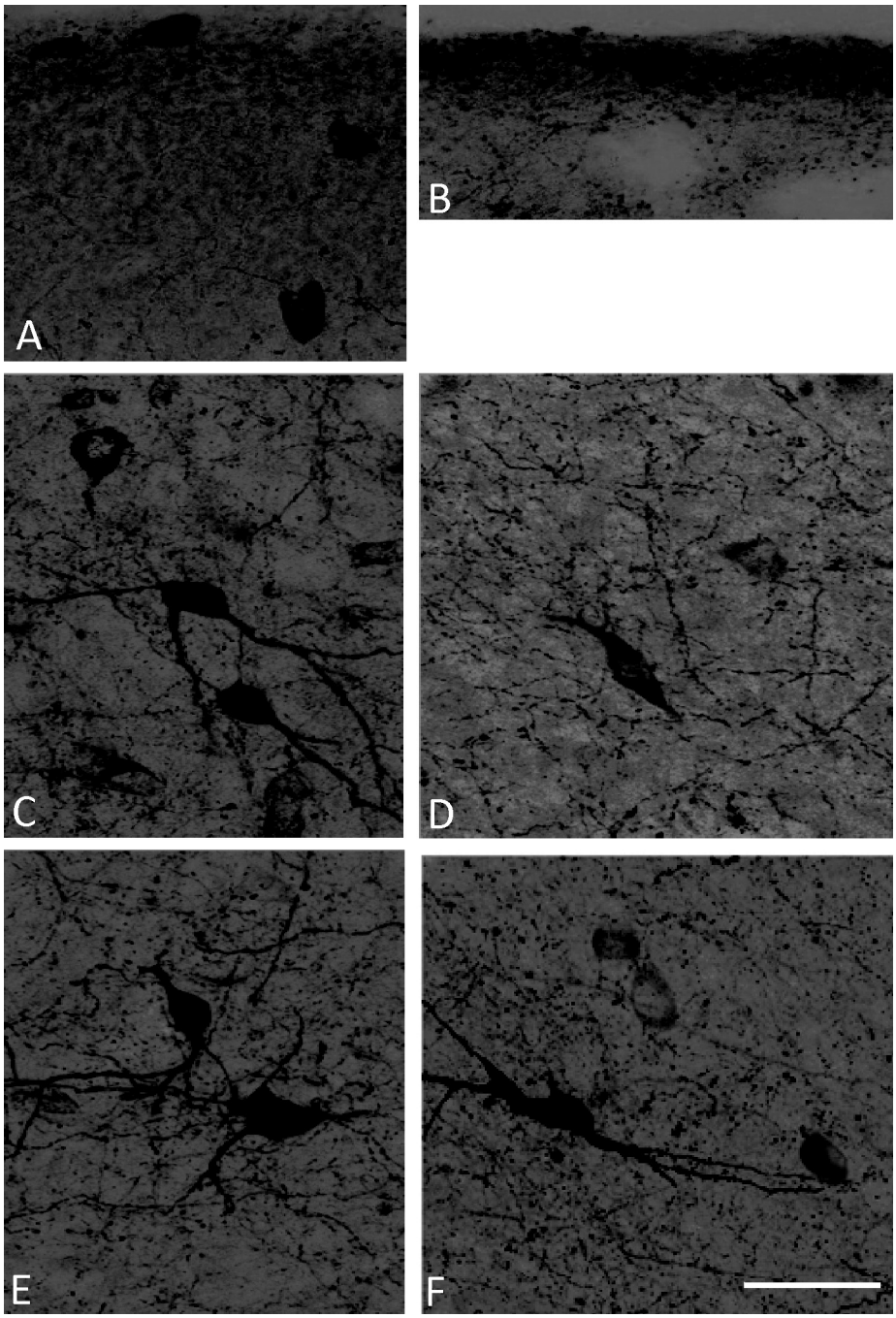
A
B
C
D
E
F

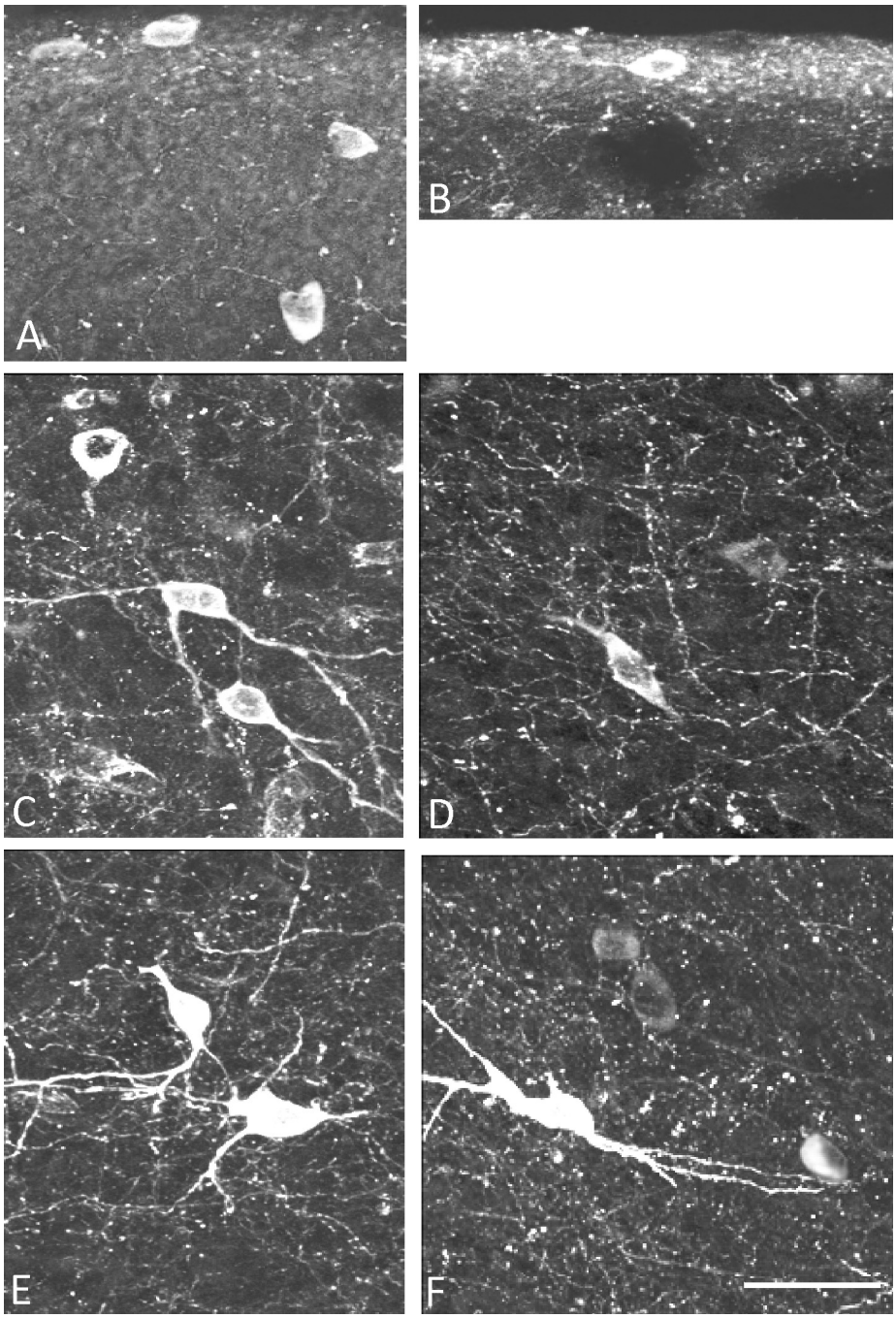

Figure 3. Photomicrographs show the interrelationships of nNOS- (red) and CR — immunoreactive elements (green) in layer I (**A**, **B**), layer II (**C**, **D**) and layer III (**E**, **F**) of the rabbit piriform cortex. Cells containing both proteins (nNOS/CR) are yellow (**A**, **B**, **D**, **F**) (scale bar — 25 μm).

that, for whatever reason, are excluded from the functional circuits [26, 27].

In the rabbit PC nNOS-ir elements show a very low level of co-localization with CR-ir elements

In the rat co-localisation of nNOS and CR within the structures neighbouring PC, specifically the claustrum, pre-endopiriform nucleus, dorsal endopiriform nucleus and ventral endopiriform nucleus, have been described previously [12, 13]. In the ventral endopiriform nucleus 64% of nNOS-ir neurons also contained CR [12]. In the main olfactory bulb of mice nNOS-ir cells also frequently contained CR [11]. Our study shows that in the rabbit PC the population of nNOS-ir Cajal-Retzius cells barely overlaps with the population of CR-ir Cajal-Retzius cells. Moreover, in

remaining parts of PC fewer than 10% of nNOS-ir neurons show CR-ir. We do not know if this situation is specific to the species or to the structure.

Experimental studies have shown that during pathological conditions, such as kindling epileptogenesis, and cerebral ischaemia, NOS mRNA expression and the number of nNOS neurons may increase by 1300% and 130%, respectively [5, 17]. It is possible that pathological conditions may modulate the synthesis of neurotransmitters in PC neurons. Further study is required to find an explanation for the neuronal nitric oxide synthase/calretinin interrelationships within the rabbit piriform cortex.

ACKNOWLEDGEMENTS

This research was supported by funds from the Ministry of Science and Higher Education, Grant ST-11.

REFERENCES

1. Ashwell KW, Phillips JM (2006) The anterior olfactory nucleus and piriform cortex of the echidna and platypus. Brain Behav Evol, 67: 203–227.
2. Badowska-Szalewska E, Klejbor I, Ludkiewicz B, Moryś J (2005) Analysis of calretinin immunoreactivity in the rat piriform cortex after open field stress during postnatal maturation. Folia Morphol, 64: 33–40.
3. Davis BJ (1991) NADPH-diaphorase activity in the olfactory system of the hamster and rat. J Comp Neurol, 314: 493–511.
4. Druga R, Kubova H, Suchomelova L, Haugvicova R (2003) Lithium/pilocarpine status epilepticus-induced neuropathology of piriform cortex and adjoining structures in rats is age-dependent. Physiol Res, 52: 251–264.
5. Elmer E, Alm P, Kokaia Z, Kokaia M, Larsson B, Keep M, Andersson KE, Lindvall O (1996) Regulation of neuronal nitric oxide synthase mRNA levels in rat brain by seizure activity. Neuroreport, 7: 1335–1339.
6. Guix FX, Uribesalgo I, Coma M, Munoz FJ (2005) The physiology and pathophysiology of nitric oxide in the brain. Prog Neurobiol, 76: 126–152.
7. Haberly LB, Price JL (1978) Association and commissural fiber systems of the olfactory cortex of the rat. J Comp Neurol, 178: 711–740.
8. Halliwell B (2002) Hypothesis: proteasomal dysfunction: a primary event in neurogeneration that leads to nitrative and oxidative stress and subsequent cell death. Ann NY Acad Sci, 962: 182–194.
9. Kara P, Friedlander MJ (1998) Dynamic modulation of cerebral cortex synaptic function by nitric oxide. Prog Brain Res, 118: 183–198.
10. Klejbor I, Ludkiewicz B, Domaradzka-Pytel B, Wójcik S, Moryś J (2005) Open field stress and neurons containing calcium-binding proteins in the piriform cortex of the rat. J Physiol Pharmacol, 56: 223–331.
11. Kosaka T, Kosaka K (2007) Heterogeneity of nitric oxide synthase-containing neurons in the mouse main olfactory bulb. Neurosci Res, 57: 165–178.
12. Kowiański P, Moryś JM, Wójcik S, Dziewiątkowski J, Luczyńska A, Spodnik E, Timmermans JP, Moryś J (2004) Neuropeptide-containing neurons in the endopiriform region of the rat: morphology and colocalization with calcium-binding proteins and nitric oxide synthase. Brain Res, 996: 97–110.
13. Kowiański P, Moryś JM, Wójcik S, Dziewiątkowski J, Moryś J (2003) Co-localisation of NOS with calcium-binding proteins during the postnatal development of the rat claustrum. Folia Morphol, 62: 211–214.
14. Kunzle H, Radtke-Schuller S (2000) The subrhinal paleocortex in the hedgehog tenrec: a multiarchitectonic characterization and an analysis of its connections with the olfactory bulb. Anat Embryol, 202: 491–506.
15. Leong SK, Ruan RS, Zhang Z (2002) A critical assessment of the neurodestructive and neuroprotective effects of nitric oxide. Ann NY Acad Sci, 962: 161–181.
16. Li J, Wu X, Dang X, Sun X, Zhao H, Hua Y (1998) Effect of +Gz-induced cerebral ischemia on the distribution of nitrix oxide synthase in rabbit brain. Space Med Med Eng (Beijing) 11: 102–106.
17. Libri V, Santarelli R, Nistico S, Azzena GB (1997) Inhibition of nitric oxide synthase prevents magnesium-free-induced epileptiform activity in guinea-pig piriform cortex neurones in vitro. Naunyn Schmiedebergs Arch Pharmacol, 355: 452–456.
18. Loscher W, Ebert U (1996) The role of the piriform cortex in kindling. Prog Neurobiol, 50: 427–481.
19. Marin-Padilla M (1998) Cajal-Retzius cells and the development of the neocortex. Trends Neurosci, 21: 64–71.
20. Mizukawa K, Vincent SR, McGeer PL, McGeer EG (1989) Distribution of reduced-nicotinamide-adenine-dinucleotide-phosphate diaphorase-positive cells and fibers in the cat central nervous system. J Comp Neurol, 279: 281–311.
21. Oermann E, Bidmon HJ, Schleicher A, Mayer B, Schwegler H, Zilles K (1998) The distribution of nitric oxide synthase-I and NADPH-diaphorase containing neurons in the cerebral cortex of different strains of mice and its association with learning and memory. J Hirnforsch, 39: 65–75.
22. Togo T, Katsuse O, Iseki E (2004) Nitric oxide pathways in Alzheimer's disease and other neurodegenerative dementias. Neurol Res, 26: 563–566.
23. Wójcik S, Dziewiątkowski J, Klejbor I, Spodnik JH, Kowiański P, Moryś J (2006) The anatomical relationships between the serotonergic afferents and the neurons containing calcium-binding proteins in the rat claustrum. Acta Neurobiol Exp, 66: 33–42.
24. Wójcik S, Dziewiątkowski J, Spodnik E, Ludkiewicz B, Domaradzka-Pytel B, Kowiański P, Moryś J (2004) Analysis of calcium binding protein immunoreactivity in the claustrum and the endopiriform nucleus of the rabbit. Acta Neurobiol Exp, 64: 449–460.
25. Wójcik S, Dziewiątkowski J, Spodnik E, Ludkiewicz B, Kowiański P, Spodnik JH, Moryś J (2004) Distribution of immunoreactivity of calcium-binding proteins in the rabbit piriform cortex. Folia Neuropathol, 42: 209–220.
26. Zhou L, Welsh AM, Chen D, Koliatsos VE (2007) NMDA inhibitors cause apoptosis of pyramidal neurons in mature piriform cortex: evidence for a nitric oxide-mediated effect involving inhibitory interneurons. Neuropharmacology, 52: 1528–1537.
27. Zhou Y, Zhou L, Chen H, Koliatsos VE (2006) An AMPA glutamatergic receptor activation-nitric oxide synthesis step signals transsynaptic apoptosis in limbic cortex. Neuropharmacology, 51: 67–76.